EXPERIMENTAL STUDY ON CHARACTERISTICS AND PERFORMANCE OPTIMIZATION OF HONEYCOMB CHARGED DUAL-ZONE ELECTROSTATIC PRECIPITATOR

by

Weijian ***HUA***[1], Yongchun ***CHU***[2], ChenYan ***YAN***[1], Guan ***WANG***[1], MinXing ***SU***[3], ZhenJie ***DING***[3], KeJie ***ZHANG***[1], RenHui ***RUAN***[1,*], XueBin ***WANG***[1,*]

1. Key Laboratory of Thermo-Fluid Science and Engineering of the Ministry of Education, School of Energy and Power Engineering, Xi'an Jiaotong University, Xi'an 710049, Shaanxi, China
2. Shaanxi Energy Zhaoshipan Coal & Electricity Co., Ltd.
3. Shanghai No.8 Nuclear Industry Research Institution, Shanghai 201800, China

Email: renhuiruan@xjtu.edu.cn, wxb005@xjtu.edu.cn

As a major air pollutant, $PM_{2.5}$ poses a serious threat to public health and the ecological environment, making the development of efficient and low-energy-consumption control technologies crucial. Two-stage electrostatic precipitators (ESP) have shown potential in $PM_{2.5}$ removal due to the separation of charging and collection processes, but traditional designs suffer from problems such as high operating voltage, large power consumption, uneven electric field distribution, and high pressure drop. In this study, a honeycomb-charged two-stage ESP was designed. The effects of honeycomb diameter, discharge needle insertion depth, charging zone voltage,collection zone voltage, and air speed on dust removal efficiency were investigated through experiments. A quality factor(Q_F) was introduced to evaluate the comprehensive performance. The results show that the optimal dust removal effect is achieved when the honeycomb diameter is 30 mm and the discharge needle insertion depth is 40 mm. Under the operating conditions of charging zone voltage of -10 kV, collection zone voltage of 8 kV, and air speed of 0.5 m/s, the removal efficiency of NaCl aerosol with particle size of less than 1 μm reaches 99.63%, the pressure drop is less than 25 Pa, the power consumption is less than 50 W, and the quality factor is 0.1179. Compared with the traditional wire-plate two-stage ESP, this design achieves a better balance between efficiency, energy consumption, and pressure drop, which can meet the $PM_{2.5}$ control requirements of industrial and indoor environments. It provides theoretical basis and technical support for the structural optimization and large-scale application of electrostatic precipitators.

Key words:*honeycomb-charged two-stage electrostatic precipitator; dust removal efficiency; quality factor(Q_F); structural optimization*

1. Introduction

Atmospheric particulate matter with an aerodynamic diameter of≤2.5 μm ($PM_{2.5}$) has become a major environmental pollutant threatening public health and ecological stability on a global scale. Epidemiological studies have demonstrated that chronic exposure to ambient $PM_{2.5}$ are associated with higher risk of developing CVDs, with a positive linear relationship, but without any safe level of exposure [1]. Moreover, some researches found the correlation between pre-natal $PM_{2.5}$ and higher rates of autism for children [2]. Recently, efforts have been taken for developing effective, energy-efficient and stable operation of emission controlling technology in order to solve the severe danger brought about by $PM_{2.5}$. Currently, mainstream $PM_{2.5}$ removal technologies include mechanical filtration, baghouse dust collection, dry ESP, WEP, and two-stage ESP, each with its own advantages and disadvantages. HEPA high-efficiency air filters are mechanical filters that can trap particles through inertialimpaction, interception, and diffusion. They may be able to sustain efficient filtering at all times but still suffer from high pressure drop etc., high energy consumption, and high cost [3]. Baghouse dust collection achieves high $PM_{2.5}$ removal efficiency (usually > 99%) using porous filter bags, but the filter bags are prone to frequent replacement due to dust accumulation, which increases maintenance costs and operational downtime [4]. Dry ESPs are extensively used in coal-fired powerplants as well as industrial boilers because of the low pressure drop and high gas volume handled by them. However, they are restricted with the lack of proper particle charging and back corona discharge can be expected for high-resistivity fly ash, which leads to the degradation of global performance [5]. The main advantages of wet ESPs are that for new designs, the system can have a pulsair-jet assisted water flow (PJWF) and hence clean in an on-line mode i.e., without stopping the operation; achieve the $PM_{2.5}$ removal efficiencies of up to 99.26% [6], and keep a stable operation time longer than 11 months under an industrial scenario. Yet conventional WEPs are characterized by a high water consumption, while sophisticated solutions might need a slightly increased initial investment as well as regular maintenance of the discharge electrode over time [6, 7]. In comparison, in a two-stage ESP, the particle charging and collecting process are separated: the charging chamber can efficiently charge the $PM_{2.5}$ via corona discharge, and the collection chamber collects charged particle with uniform dc electric field. It lowers energy use by effective charging, and enhances submicron ($PM_{2.5}$) removal efficiencies with low-pressure-drop features. Thus, it is a highly promising $PM_{2.5}$ control technology [8, 9].

In recent years, numerous advances have been made in performance optimization research of two-stage ESP, covering structural optimization, operating parameters, and reduction of energy consumption and ozone [10]. Regarding influencing factors, the geometric parameters of the precipitator directly affect ion distribution and particle charging uniformity. Munir et al. [11] investigated the effects of pre-charger geometric parameters (length, symmetry, and ionizer insertion depth) on $PM_{2.5}$ removal efficiency of a two-stage ESP-type wearable air cleaner, confirming that the cylinder-cuboid combined pre-charger achieves optimal efficiency (~98.5% at 30 L/min) while meeting strict ozone emission standards (<5 ppb). Liu *et al.* [12] developed an innovative two-stage ESP. They narrowed the electrode spacing and modified the high-voltage electrodes with a unilateral dielectric coating. This design overcomes the fundamental drawback in conventional ESPs. It increases the breakdown voltage, allowing effective particulate matter collection at very low voltage. In addition, it has good long-term stability, a small pressure drop and an ozone emission that can be controlled. Nilgumhang *et al.* [13] replaced copper discharge electrodes (rod/wire) with a tungsten-based alloy rod (2 wt.% ThO_2) in a

wire-to-cylinder electrostatic precipitator. At the optimal 10 kV voltage, the tungsten rod achieved a $PM_{2.5}$ collection efficiency of 84.1%, 5.62% higher than copper rod (78.48%) and 7.8% higher than copper wire (76.3%). It was due to its superior electrical and thermal properties as well as higher melting point, which enhanced discharge performance and particle adsorption. Honeycomb-shaped collection electrodes have been extensively studied. They stand out for their large specific surface area. They also boast uniform electric field distribution. Molchanov *et al.* [14] designed a honeycomb ESP and tested it in small-scale lignite-fired boilers.This ESP has an optimal specific collecting area of 60 $m^2 \cdot [(m^3 \cdot s^{-1})]^{-1}$ and achieved a total $PM_{2.5}$ removal efficiency ranging from 79% to 97%. Li *et al.* [15] proved that increasing the charging zone voltage, collection zone voltage, and reducing air speed could effectively increase the dust removal efficiency of two-stage electrostatic precipitator; among them, the charging zone voltage has the most significant effect on the dust removal efficiency of 0.31 μm particles. The influence of air speed on the dust removal efficiency of small-sized particles is greater than that of large-sized particles. The higher is the collection zone voltage, the better will be the performance in a limited extent and the slower it would increase after reaching some limit. In addition, the development of dual-corona pre-chargers have also increased the particle charging effect, and studies in two-stage electrostatic precipitator are now at a mature stage of technical development having achieved $PM_{2.5}$ collection efficiencies over 90%. Research should target the optimization of electrode configuration, innovation in energisation mode (i.e. pulsed, AC), integration with agglomeration or hybrid systems. These efforts aim to further reduce energy consumption and pressure drop, and expand applications in non-coal industrial sources and indoor air purification [16].

Despite significant progress in two-stage ESP research, many challenges remain for its large-scale application. Firstly, the traditional two-stage ESP must have good operational stability, high collection efficiency, and high gas treatment capacity Gas treatment capacity is limited by the following air speed limitations: air speed above about 2.4 m/s induces nonstationary particle reentrainment, leading to a temporary decrease of the collecting efciency (especially when the air speed is greater than 5 m/s, the collecting efciency of large particles with diameter larger than 5 μm decreases signifcantly). In contrast, the low air speed (≤1.4 m/s) that can avoid secondary pollution restricts the gas treatment capacity of the equipment, failing to meet the requirements of large-scale applications [17]. Second, the high voltage needed by conventional two-stage ESPs in order to reach a high particle removal efficiency may increase its energy consumption. Also, the charging stage of ESPs might have a high pressure drop (especially at high air speed) that is directly correlated with energy consumption and thus aggravate the energy-intensive drawback [12]. To overcome those issues, In this paper, we propose the two stage honeycomb ESP. It utilizes the uniform electric field and large specific surface area of the honeycomb structure to improve air flow adaptability and collection uniformity, while optimizing the parameters of the pre-charging zone and collection zone to reduce operating voltage and pressure drop.

This study investigates the key factors influencing the dust removal efficiency of the two-stage honeycomb ESP, including honeycomb diameter, discharge needle insertion depth into the charging zone, charging zone voltage, collection zone voltage, and air speed. A Scanning Mobility Particle Sizer (SMPS) was used to measure the aerosol particle removal efficiency [18]. A micro-manometer was employed to measure the pressure drop, while two built-in voltammeters of the high-voltage power supply in the charging zone and collecting zone were used to measure and calculate the energy comsuption. These data were used to evaluate the comprehensive performance of the two-stage honeycomb electrostatic precipitator. Additionally, the quality factor [19] (Q_F, an evaluation index

integrating efficiency and pressure drop) was calculated to quantify the balance between efficiency and energy consumption. The experimental results show that the relative dust removal efficiency is the highest when the honeycomb diameter is 30 mm, and the optimal efficiency is achieved when the discharge needle insertion depth is 40 mm. Moreover, the different types of honeycomb shaped two-stage electrostatic precipitators designed in this work have much better dust removal efficiencies than that of the wire plate two-stage commercial ESP bought and used as a comparison in the experiment. It is superior to that of traditional two-stage ESPs, achieving low energy consumption (< 50 W) and low pressure drop (< 25 Pa), which meets the requirements for efficient, energy-saving, and safe $PM_{2.5}$ control in industrial and indoor environments [20].

2. Materials and methods

2.1. Reagents and materials

In this experiment, analytical grade sodium chloride (NaCl, purity > 99.8%) was used to prepare a 0.35 mol/L solution, and aerosol particles were generated by an ultrasonic atomizer. The discharge needles, discharge needle brackets, charging zone plates, and collecting plates of the precipitator were all made of stainless steel. Two high-voltage DC power supplies were used to power the charging zone and collection zone. The sealing and fixing of the equipment were achieved through a cavity constructed of acrylic plates, and a hose was equipped as the exhaust gas discharge pipe.

2.2. Precipitator experimental system

Fig. 1 shows the experimental setup. An ultrasonic atomizer atomizes the prepared NaCl solution, and the generated aerosol is carried by purified compressed air (to eliminate environmental interference) into a diffusion dryer with water-absorbing silica gel for full drying. The dried particles then enter the dust removal system via an induced draft fan. We install measuring points in the inlet (nearthe precipitator) and outlet (near the exhaust pipe) of the flowchannel for ensuring stable air-flow and reliabledata. We conduct our experiment under the condition of 298 K. Circular tube near the inlet of the dust collector is with a diameter of 240 mm, and length of 30 mm, which connects with the fan exit. A circular-to-square duct with a length of 380 mm is connected behind the circular tube. The dust collector is installed in the square duct, whose cross-section is 400 mm × 400 mm. The inlet of the dust collector is 1200 mm away from the inlet of the square duct, and the outlet of the dust collector is 600 mm away from the outlet of the square duct. A square-to-circular duct is connected at the outlet of the square duct, and the tail circular tube is linked to the exhaust gas treatment device. Two sampling ports with a diameter of 20 mm were opened in the flue. The inlet sampling port is located 200 mm from the dust collector inlet, at the center of the square duct. The outlet sampling port is 400 mm away from the dust collector outlet. A flow straightening plate was also installed inside the circular-to-square duct at the flue inlet in this experiment. During the test, the anemometer was horizontally inserted into the sampling port at different depths to measure the air speed, and this procedure was repeated with varying air volumes. Experimental results show that the non-uniformity of air speed at the sampling section is less than 10%. The air speed, particle size distribution (before and after dust removal), pressure drop, and other parameters are measured sequentially to calculate the quality factor (Q_F). The quality factor (Q_F) was introduced as the evaluation metric, defined by the following equation [21]:

$$Q_F = \frac{-ln(1-\eta_T)}{\Delta P \times Q / \eta + V \times I} \quad (1)$$

where η_T is the fractional removal efficiency for specific particle sizes, ΔP is the pressure loss, Q is the flow rate, η is the fan efficiency, V is the charging voltage, and I is the charging electrode current.

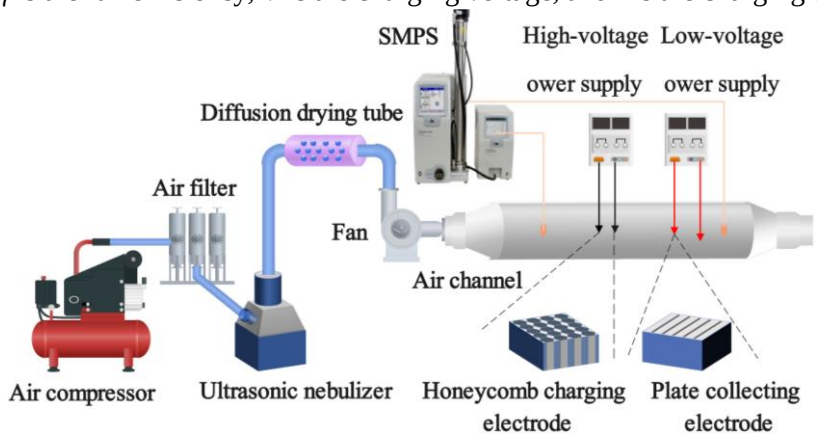

Figure 1. Experimental system for charging and dust removal characteristics of honeycomb dual-zone electrostatic precipitator.

2.3. Structure of charging module

As shown in Fig. 2, the honeycomb two-stage ESP's charging module comprises honeycomb channels, a movable bench, and 0.1 mm-diameter, 20 mm-long discharge needles. Needle insertion depth into the honeycomb (1–4 times needle length) is adjustable via the bench's screws, with the discharge needle bracket connected to a high-voltage power supply and the honeycomb structure grounded. Three honeycomb ESPs (diameters: 30/40/50 mm) were fabricated, with 163/105/68 cells and total surface areas of 3.91/3.15/2.45 m² respectively. A commercial wire-plate two-stage ESP served as the control. All honeycomb ESPs share the same collection zone as the control (wire-plate collecting plates, 12.5 mm electrode spacing, 230 mm length [15]) to eliminate interference. The wire-plate ESP's charging zone has the same plate length as honeycomb ESP's and matches the 50 mm honeycomb's electrode spacing. Its charging zone uses 4 stainless steel serrated electrodes (total area 0.2442 m², Fig. 2(a)). The mass removal efficiency was compared across groups under identical operating conditions.

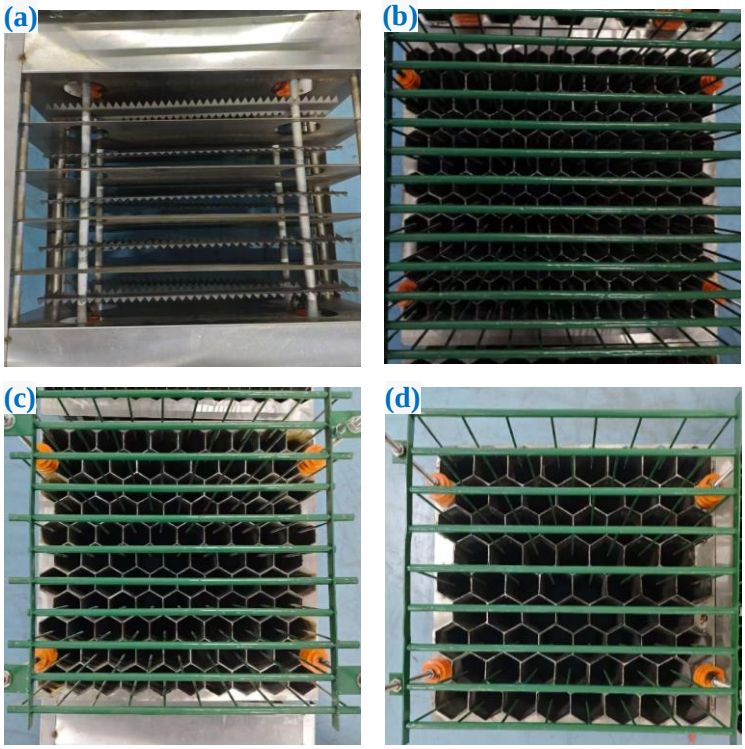

Figure 2. Charging module of dual-zone electrostatic precipitator. (a) Aditional wire-plate charging module; Honeycomb charging modules with different cell diameters: (b) 30 mm; (c) 40 mm (d) 50 mm

2.4. Measurement of aerosol particle size

A SMPS was used to measure the particle size distribution of the aerosol particles after atomization and drying by the diffusion dryer. The number distribution of NaCl aerosol particles was obtained, and the mass distribution of corresponding particle sizes was calculated based on the relationship between number and mass (During the calculation, the particle shape is assumed to be cubic). The measurement and calculation results are shown in Fig. 3. It can be seen that the particle size corresponding to the peak number concentration does not coincide with that of the peak mass concentration, and the peak mass concentration is mainly concentrated in large-sized particles.

Based on the statistics and counting of particle size distribution, the dust removal efficiency of the electrostatic precipitator can be calculated [22]:

$$\eta_1 = (1 - \frac{c_{out}}{c_{in}}) \times 100\% \quad (2)$$

where c_{out} is the mass concentration of particles at the outlet of the precipitator, and c_{in} is the mass concentration of particles at the inlet of the precipitator. Before calculating the removal efficiency, the particle size distribution in the environment was measured, and all experimental results have excluded the influence of the experimental environment. Each group of experiments was repeated more than three times.

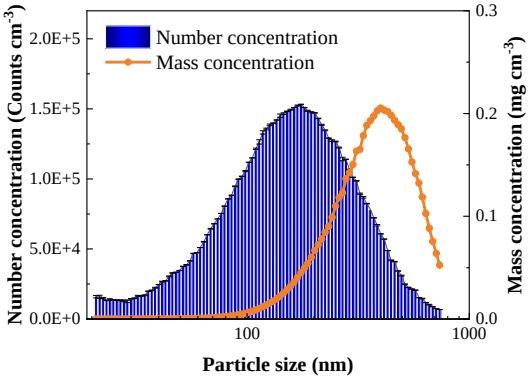

Figure 3. Particle size distribution of NaCl aerosol.

3. Results and discussion

3.1. Volt-ampere characteristics and power consumption

Negative high voltage applied to the ESP's charging electrode breaks down air, generating electrons that attach to electronegative species to form charged ions. These ions and electrons collide with particles to charge them via field charging (electric field-driven, saturated) or diffusion charging (ion thermal motion-driven) [16]. Han *et al.* [23] noted field and diffusion charging act synergistically for 20–200 nm particles. Charged particles move toward the opposite-polarity grounded electrode under electric field force and are collected. Key factors affecting ESP efficiency are particle charging performance and residence time. Volt-ampere characteristics of the charging module affects the charging performance of particles. The experiment focused on a wire-plate two-stage ESP (FESP) and honeycomb two-stage ESPs (HESP) with 30/40/50 mm diameters, using a DC high-voltage power supply for constant voltage application. The volt-ampere and power characteristics of the charging zone are shown in Fig. 4(a): The power draw was largest with the 30 mm HESP (up to 44 W at -10 kV, limited by the protection device) because of its small distancebetween the discharge needle and ground electrode. This willenhance the electric field strength and current density. By contrast, the 50 mm HESP exhibited the lowest power consumption, which is slightly lower than that of the FESP. This is caused by two key factors: first, it has the same charging electrode spacing as the FESP; second, its radially uniform, closed internal structure generates a stable electric field. The stable electric field helps reduce energy loss [24]. Fig. 4(b) shows the relationship between dust removal efficiency and power (collection zone voltage: 8 kV positive high voltage, air speed: 1 m/s). Beyond 28 W, the particle removal efficiency barely increased, indicating saturated charging of NaCl aerosols. At the same power, the 30 mm HESP achieved the highest dust removal efficiency. The reduced size of its diameter decreased the discharge needle-plate distance that further increased electric field strength and space charge density leading to an increase in the effective charging area due to a combined effect.finally leading to a better charge transfer of particles. In addition, due to the small electrode spacing more charged particles were captured within the charging zone, further increasing the efficiency [25]. All HESPs outperformed the wire-plate ESP in dust removal efficiency.

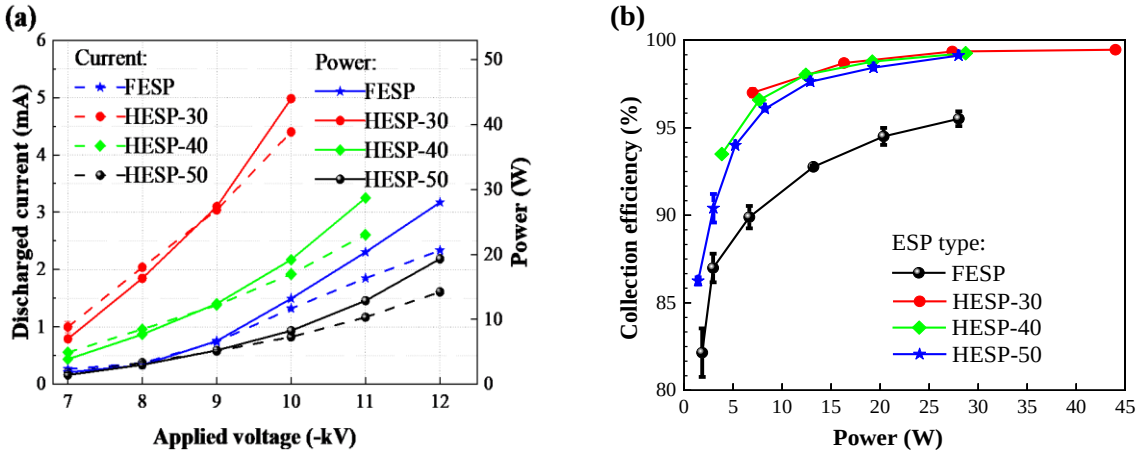

Figure 4. (a) Volt-ampere characteristic curves and power of charging zones; (b) Relationship between removal efficiency and power of charging zones

3.2. Effect of discharge needle insertion depth

The research object is a honeycomb two-stage electrostatic precipitator with a diameter of 50 mm, and to study the influence of discharge needle position on the dust removal rate. the lengths of the discharge needle inserted into the charging region were respectively selected as 20 mm, 40 mm, 60 mm, and 80 mm, and other operation parameters are determined by keeping them constant with values including an air speed at 1 m/s, charging power of 28W (Voltage on the charge area: -12 kV), and collection zone voltage of 8 kV. According to the particle size distribution, the number concentration median diameter of NaCl aerosol is approximately 150 nm, while the mass concentration median diameter is approximately 400 nm. The dust removal efficiency as a function of discharge needle insertion depth are presented in Fig. 5(a). It can be observed from this figure that the particle removal efficiency is least effective on particles with diameters of between 100 nm and 200 nm, while the dust removal efficiencies of the representative particles (of diameter 100nm, respectively), where the dashed lines (solid circles with error bars) correspond to a thickness of 150 nm, and 400 nm, respectively, which is plotted in Fig. 5(b). At a discharge needle penetration depth at the charging region of 40 mm, the overall mass removal efficiency of the NaCl aerosol reaches at maximum value of 98.51% (for particle size 400 nm). It is worth noting that the removal efficiency for the 100 nm particle—the so-called most difficult-to-catch particle—is also above 85% indicating good high-efficiency dust removal capability of the system. In particular, almost 100% removal efficiency can be obtained in a range of particle mass (i.e., diameter larger than 4000 nm), which further confirms the effectiveness of the proposed structure. Insertion depth will affect the electric field intensity as well as its uniformity. Too deep an insertion depth would cause low enough electric field, whereas a too large penetration depth leads to the saturation of the electric fields (or its distortion). An appropriate insertion depth allows the space charge to overlap with the peak electric field, thereby achieving sufficient particle charging[26].In addition, the insertion depth also influences the effective charging time of particles. If the insertion is too deep, some charged particles leave the charging region before being captured by the collecting plates, which reduces the dust removal efficiency of the plates in the charging zone [9].

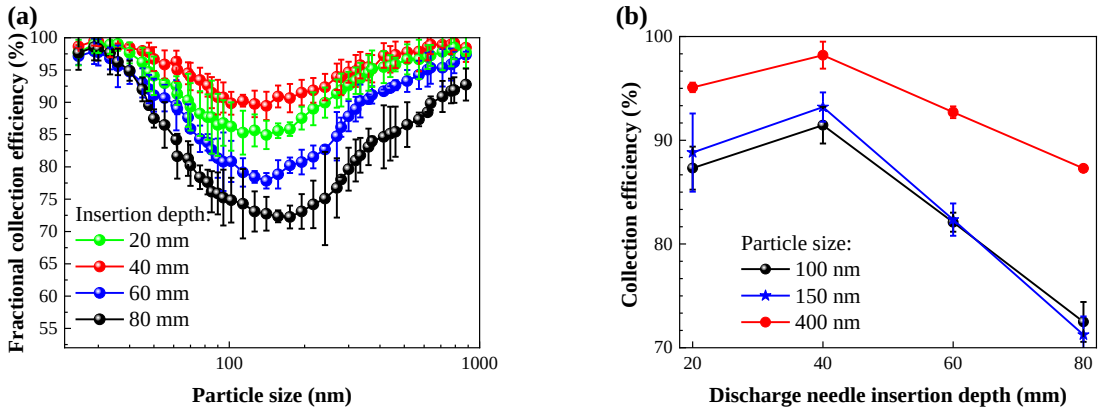

Figure 5. Dust removal efficiency of submicron particles for a HESP-50 collector. (a) as a function of particle size for different needle insertion depths; (b) as a function of needle insertion depth for different particle sizes

3.3. Effect of collection zone voltage

Selected honeycomb electrostatic precipitator with a diameter of 30 mm, 40 mm and 50 mm as research object. Discharge needle insert depth in charge region is set to be 40 mm, with air speed and charging power of 1 m/s and 28 W, respectively. The results shown in Fig. 6(a) were obtained by varying the collection zone voltage. As the collection zone voltage increases, the particle removal efficiency increases correspondingly. However, when the collection zone voltage reaches 9 kV, the dust removal efficiency decreases slightly. Fig. 6(b) illustrates the dust removal efficiency of the 30 mm-diameter HESP at different collection zone voltages(The voltage applied to the charged region is -10 kV.). It is worth noting that good removal efficiencies of 100 nm particles occur at a collection zone voltage setting of 7 kV and 8 kV. Based on the dust removal efficiency result, a distinct breakdown phenomenon appears at the collection zone voltage around 9 kV, which breaks down the stable V–I characteristic and the homogeneous current density distribution. both of which are necessary conditions for successful particle charging and migration. In particular, breakdown causes a runaway growth of the ionisation region resulting in deformation of the electric field which reduces the effectiveness of both particle charging and migration. On the other hand,breakdown induced flow perturbations further deteriorates the dust removal efficiency [27].

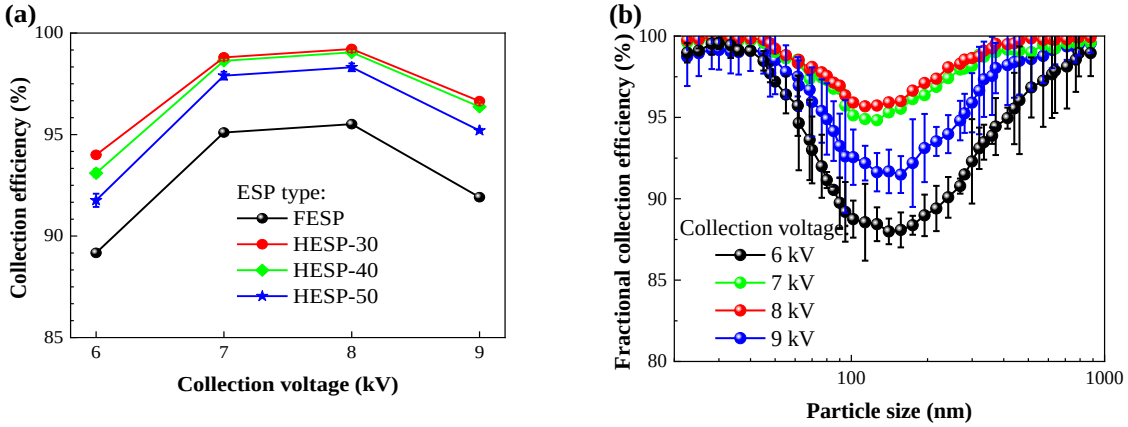

Figure 6. Dust removal efficiency of submicron particles. (a) as a function of collection voltage for different ESP types; (b) as a function of particle size at different collection voltages for a HESP-30 collector.

3.4. Effect of charging zone voltage

Three different diameter honeycomb two-stage ESPs (HESP) i.e., 30 mm, 40 mm, and 50 mm, as well as the wire-plate two stage ESP (WP-TSEP), were used as samples for study. The discharge needle inserting distance of charging area is set as 40 mm, air speed and collecting zone voltage are respectively 1 m/s and 8kV, respectively. The experimental data obtained by sweeping the charge region voltage are shown in Fig. 7(a). The overall mass removal efficiencies increase accordingly to the rise in charging voltage while the highest possible charging voltage was limited by the HESP diameter: -10kV (for the 30 mm diameter HESP) and -11kV (for the 40 mm diameter HESP). Higher than this voltages caused a serious breakdown associated with specific electric sparks.

Fig. 7(b) illustrates the fractional removal efficiency at different charging zone voltages under the conditions of a 30 mm-diameter HESP and an 8 kV collection zone voltage. Notably, high removal efficiencies for the refractory 100 nm particles are achieved when the charging zone voltage is set to -9 kV and -10 kV. Additionally, an obvious saturation phenomenon is observed in the effect of charging zone voltage on removal efficiency. This behavior can be attributed to the inherent upper limits of field charging and diffusion charging mechanisms: the charge quantity of particles cannot accumulate infinitely and reaches a saturation state at a certain charging voltage [16].

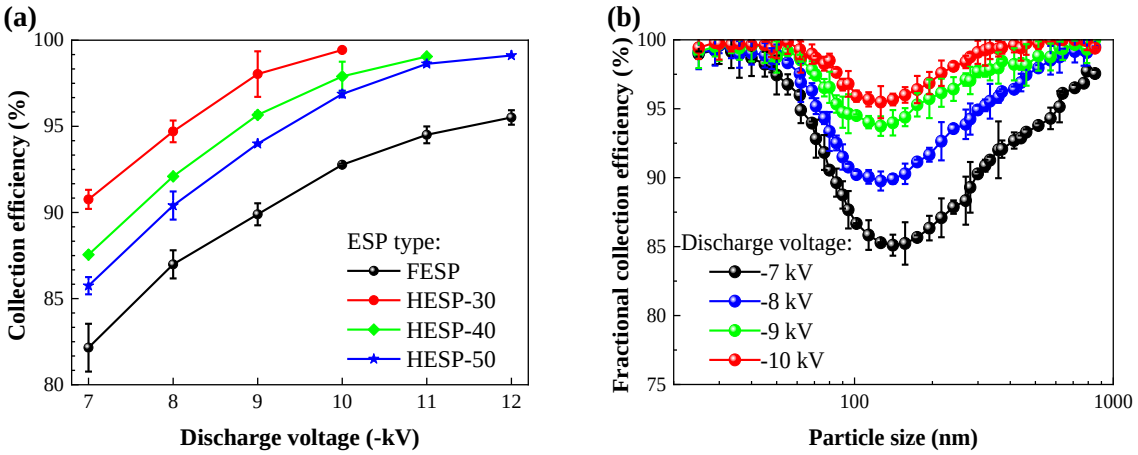

Figure 7. Dust removal efficiency of submicron particles. (a) as a function of discharge voltage for different ESP types; (b) as a function of particle size at different discharge voltages for a HESP-30 collector.

3.5. Effect of air speed

The test objects were honeycomb two-stage electrostatic precipitators (HESPs) with diameter 30 mm, diameter 40 mm, diameter 50 mm. As well as a wire-plate two-stage electrostatic precipitator (WP-TSEP). The discharge needle insertion depth in the charging zone was fixed at 40 mm, with the charging power and collection zone voltage set to 28 W and 8 kV, respectively. The efficiency for dust collection in various air speeds is shown in Fig. 8(a). Low air speed increases the retention time of charged particles inside the precipitator, thus increasing their capture rate, as well as the total dust removal performance. The 40 mm diameter HESP has best performance among all tested configuration. The dust removal efficiency of the 30 mm diameter HESP with a charging power of 44 W is shown in Fig. 8(b) (Voltage applied on charged zone is -10 kV). When the air speed is 0.5 m/s, the total residence time of particle in precipitator is about 0.76s and the highest total dust collection rate reaches to 99.63%, especially, removal efficiencies of almost 100 % were achieved at particle sizes between 20-50 nm and 500-1000

nm. A sharp decrease of removal efficiencies occurred at air speeds higher than 2 m/s. The dust removal efficiency of the 100 nm particles decreased to about 80 %, which would negate the inherent advantage of two stage electrostatic precipitators in removing submicron sizedparticles with a high dust removal efficiency.

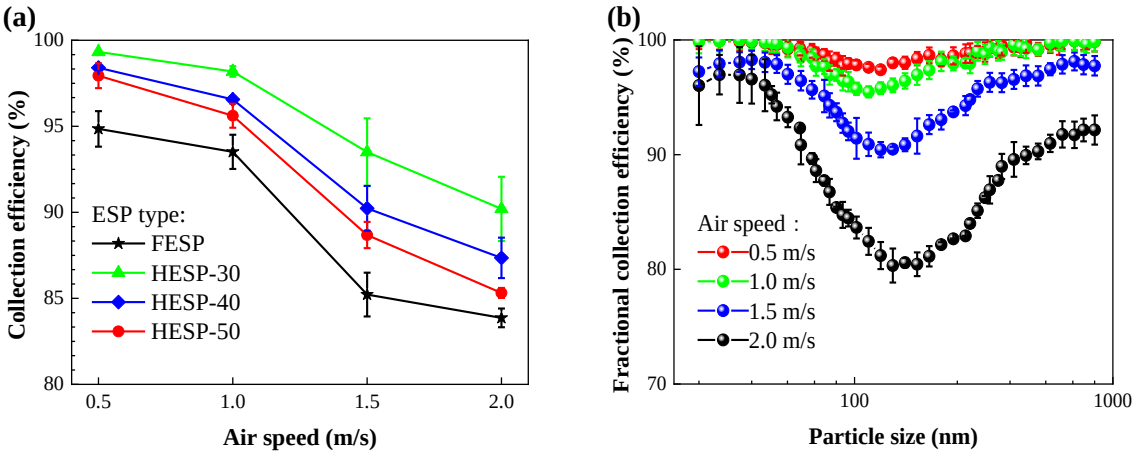

Figure 8. Dust removal efficiency of submicron particles. (a) as a function of air speed for different ESP types; (b) as a function of particle size at different air speeds for a HESP-30 collector.

3.6. Quality factor

As shown in Fig. 9, at the same working condition, the HESP with diameter of 30 mm has the best overall performance. As the input power of the HESP increases from 20 W to 28 W, the related QF increased correspondingly. In comparison, the QF of the FESP reduced with the same power raise, which mainly resulted from the reason that the rising speed of dust removing effectiveness is less than the increasing speed of power consumption. In a similar way, when we further increased the power of the 30 mm-diameter HESP to 44 W, it's QF also declined with the same reason as above. It shows that in the optimization of electrostatic precipitator, the simultaneous optimization on both the dust removal efficiency and the consumed energy is necessary for an overall better performance.

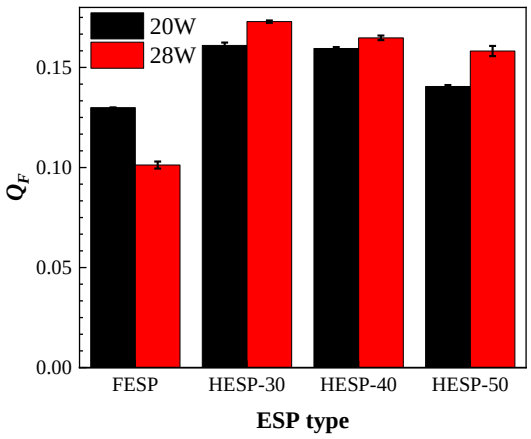

Figure 9. Performance comparison of different electrostatic precipitators.

4. Conclusions

This paper comparatively analyzed the submicron particles collection efficiency and energy

consumption between different diameter of self-developed hexagonal two stage electrostatic precipitator (HESPs) and traditional wire plate electrostatic precipitator (WP-TSEP), which proved the better dust removal effect in hexagonal two stage electrostatic precipitator. Moreover, we varied the effectiveness of dust cleaning according to important parameters such as the penetration length of the discharge needle, charging electrode voltage, collection region voltage and air speed in HESP, thus provides theoretical and experimental foundation for the structural optimized design of electrostatic precipitator.

(1) The highest dust removal efficiency of HESPs was achieved when the discharge needle insertion depth is twice the needle length. The impact of the honeycomb diameter is greater than the discharge needle insertion depth on the dust removal efficiency. A smaller honeycomb diameter resulted in smaller electrode spacing and higher current density. This led to higher power consumption at the same applied voltage. Due to breakdown limitations, the maximum applicable voltage on the charging electrode was lower.

(2) Increasing the charging zone voltage enabled more particles to be charged, improving dust removal efficiency. Increasing the collection zone voltage enhanced the deflection electric field, providing greater driving force for charged particles and improving dust removal efficiency. When breakdown happened, the charging and collection capabilities were affected, leading to a significant decrease in dust removal efficiency. Reducing the air speed effectively increased the residence time of particles in the precipitator, significantly enhanced dust removal efficiency. When designing the precipitator, the stability of the internal flow field should be considered to reasonably increase the residence time of particles in the precipitator.

(3) While the 30 mm-diameter HESPs have a higher power consumption with the same voltage, it showed the highest quality factor in the same power. Remarkably, a higher god did not lead to a higher quality factor. When selecting the operation regime for the precipitator, one must consider the value of the quality factor so as to operate the precipitator at the most efficient point, maximizing a goal of high efficiency and energy saving.

Acknowledgment

This research was supported by the Innovative Scientific Program of CNNC.

References

[1] Liu, C., K.H. Chan, J. Lv, *et al.*, Long-Term Exposure to Ambient Fine Particulate Matter and Incidence of Major Cardiovascular Diseases: A Prospective Study of 0.5 Million Adults in China, *Environmental Science & Technology*, *56*. (2022), 18, pp. 13200-13211

[2] Yu, X., M.M. Rahman, J.C. Lin, *et al.*, The potential effects of hypothetical PM2. 5 interventions on childhood autism in different neighborhood socioeconomic contexts, *American Journal of Epidemiology*. (2025), p. kwae462

[3] Niu, Z., Q. He, C. Chen, A PM2.5 pollution-level adaptive air filtration system based on elastic filters for reducing energy consumption, *Journal of Hazardous Materials*, *478*. (2024),

[4] Xia, S., L. Duan, J. Wang, *et al.*, Effect of the Surface Treatment Process of Filter Bags on the Performance of Hybrid Electrostatic Precipitators and Bag Filters, *Atmosphere*, *13*. (2022), 8

[5] Huang, Y., S. Li, Q. Zheng, *et al.*, Recent progress of dry electrostatic precipitation for PM2. 5 emission control from coal-fired boilers, *Int. J. Plasma Environ. Sci. Technol*, *9*. (2015), 2, pp. 69-95

[6] Lu, H.-H., T.-C. Le, T.-S. Tsai, *et al.*, Toward near-zero emission control technology for SO2, PM2.5 and white smoke in the steel industry, *Process Safety and Environmental Protection*, *202*. (2025),

[7] Lu, H.-H., C.-P. Lin, T.-C. Le, *et al.*, Novel wet electrostatic precipitator using pulse-air-jet-assisted water flow (PJWF) for online dust cake removal, *Separation and Purification Technology*, *367*. (2025),
[8] Jaworek, A., A. Marchewicz, A.T. Sobczyk, *et al.*, Two-stage electrostatic precipitator with dual-corona particle precharger for PM2.5 particles removal, *Journal of Cleaner Production*, *164*. (2017), pp. 1645-1664
[9] Zhu, Y., C. Chen, J. Shi, *et al.*, Experimental investigation of the effect of collection length in a two-stage electrostatic precipitator for removal of PM2.5, *Chemical Engineering Journal*, *421*. (2021),
[10] Zhu, Y., Z. Wei, X. Yang, *et al.*, Comprehensive control of PM 2.5 capture and ozone emission in two-stage electrostatic precipitators, *Science of The Total Environment*, *858*. (2023),
[11] Munir, M.H., S. An, G. Lee, *et al.*, Effects of pre-charger length, symmetry and insertion depth on PM2.5 removal efficiency for electrostatic precipitator (ESP)-type wearable personal air cleaner, *Journal of Electrostatics*, *135*. (2025),
[12] Liu, X., Y. Gao, J. Mo, *et al.*, Sub-kilovolt electrostatic precipitation for efficient and safe removal of airborne particles, *Separation and Purification Technology*, *361*. (2025),
[13] Nilgumhang, K., S. Sulaiman, K. Komnoi, *et al.*, Effect of Discharge Electrode Material on Dust Collection for Electrostatic Precipitator Efficiency, *Current Applied Science and Technology*. (2025),
[14] Molchanov, O., K. Krpec, J. Horák, *et al.*, Specifics of Electrostatic Precipitation of Fly Ash from Small-Scale Fossil Fuel Combustion, *Processes*, *11*. (2023), 3
[15] Li, S., S. Zhang, W. Pan, *et al.*, *Experimental and theoretical study of the collection efficiency of the two-stage electrostatic precipitator*, *Powder Technology*. 2019. p. 1-10.
[16] Jaworek, A.,K. Adamiak, Recent progress in research on electrostatic precipitation (invited paper), *Journal of Electrostatics*, *137*. (2025),
[17] Islamov, R.S., Analysis of the dynamics of dust reentrainment with simultaneous electrostatic deposition and without any deposition after a jump of airflow velocity, *Journal of Aerosol Science*, *144*. (2020),
[18] Zhang, B., L. Brown, I. Aravind, *et al.*, Asymmetric remediation of soot particles in a bipolar electrostatic precipitator using transient plasma discharge, *Aerosol Science and Technology*, *59*. (2025), 12, pp. 1545-1552
[19] Feng, Z., W. Pan, H. Zhang, *et al.*, Evaluation of the performance of an electrostatic enhanced air filter (EEAF) by a numerical method, *Powder Technology*, *327*. (2018), pp. 201-214
[20] Park, D., T. Kim, S. Kim, *et al.*, Impact of Ventilation Type on Bc, Pm2. 5, and Co2 Concentrations in Urban Residential Buildings: A Case Study in South Korea.
[21] Lee, Y., Y.-S. Kim, H. Lee, *et al.*, Retrofitting of an Air Handling Unit by a Two-Stage Electrostatic Precipitator, *IEEE Transactions on Industry Applications*, *60*. (2024), 1, pp. 1656-1664
[22] Han, B., H.j. Kim, Y.j. Kim, Fine particle collection of an electrostatic precipitator in CO2-rich gas conditions for oxy-fuel combustion, *Science of The Total Environment*, *408*. (2010), 21, pp. 5158-5164
[23] Han, B., H.-J. Kim, Y.-J. Kim, *et al.*, Unipolar Charging of Fine and Ultra-Fine Particles Using Carbon Fiber Ionizers, *Aerosol Science and Technology*, *42*. (2008), 10, pp. 793-800
[24] Zheng, C., Y. Wang, X. Zhang, *et al.*, Current density distribution and optimization of the collection electrodes of a honeycomb wet electrostatic precipitator, *RSC Advances*, *8*. (2018), 54, pp. 30701-30711
[25] Ouatah, E.H., S. Megherfi, B. Bendahmane, *et al.*, Effect of Room's Temperature and Electrode Gap on Current of Negative Corona Discharge in Rod-Plane Electrode Configuration, *Mathematical Modelling of Engineering Problems*, *9*. (2022), 2, pp. 298-304
[26] Kawada, Y., H. Shimizu, A. Zukeran. *Considerations of suitable grounded electrode length of pre-charger in two-stage-type electrostatic precipitator*,2017 IEEE Industry Applications Society Annual Meeting,2017, pp. 1-7
[27] Zhao, H., G. Yang, J. Shen, *et al.*, Research on the shielding effect of the electrode frames in the electrostatic precipitator, *Journal of the Air & Waste Management Association*, *73*. (2023), 6, pp. 462-470

Submitted: 30.12.2025.
Revised: 06.03.2026.
Accepted: 07.03.2026.